

13.1

Synthesis of ZnO epitaxial films at room temperature with high growth rates by direct current magnetron sputtering

© A.M. Ismailov¹, T.A. Guidalaeva¹, A.E. Muslimov², M.R. Rabadanov¹, M.Kh. Rabadanov¹

¹Dagestan State University, Makhachkala, Dagestan Republic, Russia

²Shubnikov Institute of Crystallography, Kurchatov Complex of Crystallography and Photonics, National Research Center „Kurchatov Institute“, Moscow, 123182 Russia
E-mail: egdada@mail.ru

Received January 10, 2024

Revised April 28, 2024

Accepted May 24, 2024

ZnO ceramic target ((0001)ZnO || (11 $\bar{2}$ 0)Al₂O₃) epitaxial films with record-high growth rates (7 nm/s) and low epitaxy temperatures (35°C) were obtained on sapphire substrates by direct current magnetron sputtering in an oxygen environment. It was found that an optimal substrate location in the magnetron plasma region, corresponding to a floating potential value of 9–12 V on the substrate, is a necessary condition for the growth of ZnO epitaxial films.

Keywords: ZnO, epitaxial films, magnetron sputtering method, film growth rate, sapphire substrates.

DOI: 10.61011/TPL.2024.09.59156.19861

Owing to a unique combination of physicochemical properties and a wide range of practical applications (piezoelectric transducers, ultraviolet photodetectors, gas sensors, transparent conducting electrodes, flexible thin-film diodes and transistors, etc. [1–4]), zinc oxide (ZnO) remains an appealing wide-gap semiconductor material. Despite the rapid progress in growth technology, industrial-scale growth of bulk zinc oxide crystals [5] and consequently, ZnO substrates is still infeasible. This is the reason why ZnO films and layers for device structures to be used in practice are grown mostly by vapor deposition on foreign substrates [6–9]. Owing to its simplicity, versatility, scalability, and the potential to control the composition and microstructure of the deposit, magnetron sputtering has become the most widely used method for deposition of ZnO of various functionality.

Only a relatively small number of the multitude of studies on growth of ZnO thin films by magnetron sputtering are focused on epitaxial growth [10–16]. This is attributable to the fact that a polycrystalline ZnO film structure is sufficient in many applications. For example, a resistivity of $\sim 10^{-3}$ – 10^{-4} $\Omega\cdot\text{cm}$ and a transparency of ~ 80 – 90% , which are quite acceptable for commercial production [17], were achieved for ZnO films used as transparent and conductive coatings for polycrystalline films doped with group III impurities. In contrast, epitaxial (or highly oriented) ZnO films are needed when they are used as active elements of acoustoelectric and acoustooptic devices (such as filters, surface acoustic wave (SAW) sensors [1,18,19], and deflectors [20]), since ZnO films oriented along axis c exhibit strong piezoelectric and piezooptic properties.

In most cases, the structure of films deteriorates as the deposition rate increases and the substrate temperature decreases. Threshold values of the substrate temperature

and the epitaxial growth rate are defined as the minimum temperature (at a given low growth rate) and the maximum growth rate (at a given high temperature) at which a single-crystal film may still be grown. Literature values of threshold growth rates of epitaxial ZnO films obtained by magnetron sputtering do not exceed 0.3 nm/s [21]. The threshold temperature of ZnO epitaxy on sapphire was reported to be 300°C at deposition rates of 0.025 nm/s [21]. A threshold epitaxy temperature of 80°C was achieved at a growth rate of 0.0125 nm/s in experiments on reactive magnetron sputtering of a zinc target [12].

We have established earlier [22] that a necessary condition for high-rate (7 nm/s) growth of highly oriented ZnO films on an amorphous substrate (SiO₂/Si) is its optimal positioning in magnetron discharge plasma corresponding to a floating potential of 9–12 V. In continuation of this research, an amorphous substrate was replaced by a single-crystal (11 $\bar{2}$ 0)Al₂O₃ one, which allowed us to investigate the patterns of epitaxial growth reported below.

The experimental procedure of ZnO film deposition was detailed in [22]. Rectangular sapphire samples 12 × 15 × 0.3 mm in size cut out of two-inch (11 $\bar{2}$ 0)Al₂O₃ wafers (Monocrystal PLC, Russia) were used as substrates. Since these substrates were epi-ready, no pre-treatment was performed prior to growth. Films were deposited onto substrates through a mask (8 × 8 mm); the ZnO film thickness non-uniformity within this area was 5% for a film with a thickness of 1.5 μm . The growth rate was estimated based on the film thickness determined from SEM (scanning electron microscopy) images of transversely cleaved samples and the deposition time.

X-ray diffraction (XRD) was used for structural studies of films. XRD patterns were recorded with an Empyrean PANalytical (Netherlands) diffractometer in the Bragg–

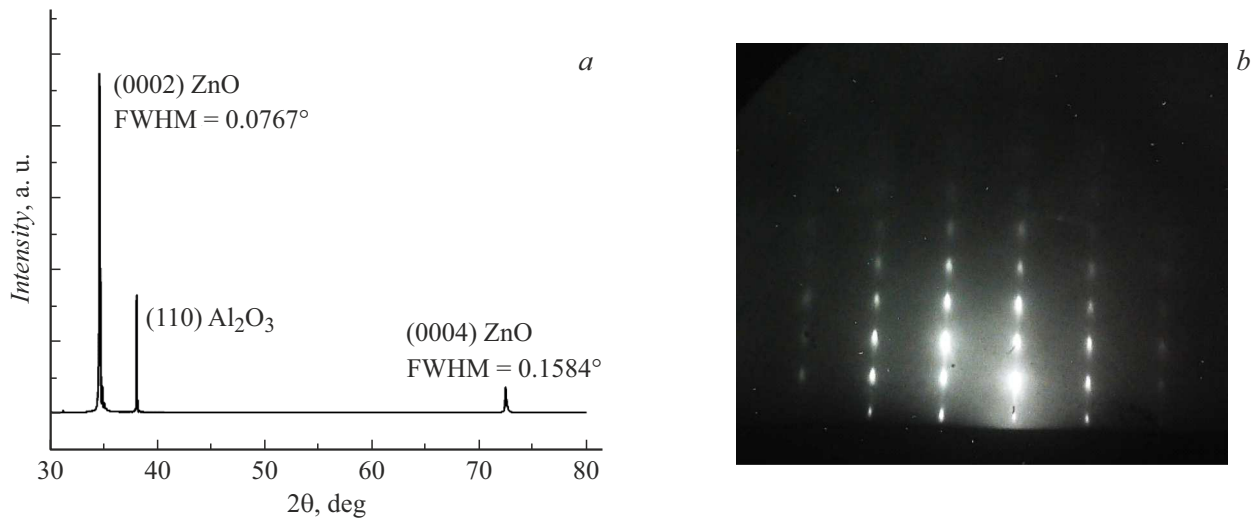


Figure 1. *a* — XRD pattern of an epitaxial ZnO film; *b* — reflection electron diffraction pattern for an epitaxial ZnO film (the electron energy is 75 keV).

Brentano reflection geometry ($\omega-2\theta$ geometry). Copper anode radiation ($\text{CuK}\alpha_2$ radiation, $\lambda = 1.5406 \text{ \AA}$) was used. Reflected high-energy electron diffraction (RHEED) with an EG-75 electron diffractometer (Russia) was also used for qualitative assessment of the structural perfection of ZnO films. The surface morphology of samples was examined with an Ntegra Spectra atomic force microscope (NT-MDT, Russia).

The size of crystallites in a ZnO film was estimated using the Scherrer equation: $D = 0.9\lambda/\beta \cos \theta$, where D is the average grain size [nm], λ is the X-ray radiation wavelength [nm], and β is the diffraction peak FWHM [rad].

Figure 1 presents the XRD pattern (*a*) and the reflection electron diffraction pattern (*b*) for a ZnO film synthesized at substrate temperature $T_s = 500^\circ\text{C}$, discharge current density $j = 120 \text{ mA/cm}^2$, pressure (oxygen) $p = 1.33 \text{ Pa}$, and deposition time $t = 3 \text{ min}$. The film thickness is $h = 1.26 \text{ }\mu\text{m}$, and the growth rate is $v = 7 \text{ nm/s}$.

It can be seen from Fig. 1, *a* that two peaks at angles 2θ of 34.50173° and 72.46367° correspond to reflections (0002) and (0004) from the (0001)ZnO basal plane, while the peak at $2\theta = 37.97682^\circ$ corresponds to the (11 $\bar{2}$ 0)Al₂O₃ substrate. This implies that basal plane (0001) of zinc oxide is parallel to the (11 $\bar{2}$ 0)Al₂O₃ substrate surface; i.e., the (0001)ZnO || (11 $\bar{2}$ 0)Al₂O₃ condition is satisfied. This is also confirmed by indexing of the reflection electron diffraction pattern in Fig. 1, *b*. The high intensity of peak (0002) and its full width at half maximum (FWHM), which is equal to 0.0767° , are indicative of a high degree of structural perfection of the obtained films. The average crystallite size determined by the Scherrer formula for the (0002)ZnO peak is 108 nm. The interplanar distance for $2\theta = 34.50173^\circ$ may be calculated using the Wulff–Bragg formula: $d_{(0002)} = 2.59738 \text{ \AA}$. Lattice parameter c and interplanar distance $d_{(0002)}$ for the hexagonal

(wurtzite) structure of ZnO are related as $c = 2d_{(0002)}$. Calculations yield the following value for the film: $c_{\text{film}} = 5.19476 \text{ \AA}$. The calculated strain in the film along axis c is $\varepsilon = (c_{\text{film}} - c_{\text{bulk}})/c_{\text{bulk}} = -0.0023$ (0.23%), where $c_{\text{bulk}} = 5.20660 \text{ \AA}$ is the parameter for a bulk (unstrained) ZnO crystal.

The shape of crystallites in the film is indicated by vertical extension of diffraction reflections in the electron diffraction pattern (Fig. 1, *b*). It is known that a reciprocal lattice node (diffraction reflection) extends in the direction parallel to the smallest dimension of a crystal. In the RHEED geometry, this is the direction perpendicular to the substrate. Therefore, crystallites are plate-shaped and arranged parallel to the substrate. The minus sign of strain ε corresponds to compressive strain along crystallite axis c . An increase in substrate temperature leads to a gradual reduction of the magnitude of reflection extension in RHEED patterns; at $T_s = 650\text{--}800^\circ\text{C}$, point reflections are observed, indicating a transition from plate-shaped crystallites to their columnar form.

A record-low (near-room) epitaxial growth temperature of $T_{s \text{ min}} = 35^\circ\text{C}$ was achieved at high growth rates of 2.8 nm/s (Fig. 2). However, it should be noted that this substrate temperature cannot be maintained for a long time due to the proximity of the substrate to the sputtered target (3.5 cm): the substrate temperature at the end of deposition (30 min) reached 200°C . Nevertheless, the specified temperature may still be regarded as minimal at this point, since the outcome of epitaxial growth is determined entirely by its initial stage, which proceeds at a temperature of 35°C . This temperature value is hardly a threshold, since it arises from technical limitations and is not stipulated by the processes of epitaxial growth. The high growth rate of ZnO epitaxial films (7 nm/s) is also not the limit (threshold) one above which epitaxiality is lost.

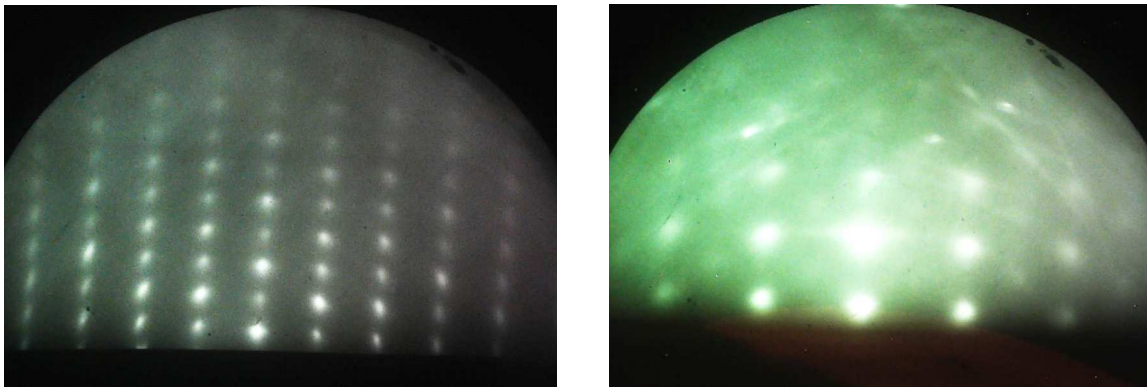


Figure 2. Reflection electron diffraction patterns recorded at two different azimuth angles for an epitaxial ZnO film obtained at a temperature of 35°C , $j = 33 \text{ mA/cm}^2$, $t = 30 \text{ min}$, $h = 5 \mu\text{m}$, and $v = 2.8 \text{ nm/s}$.

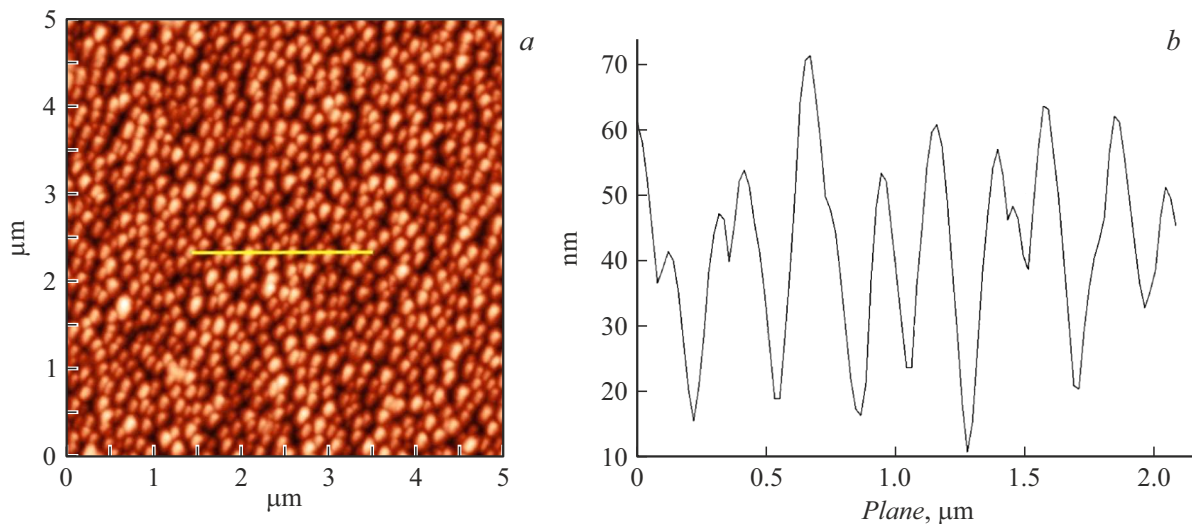


Figure 3. *a* — surface topography of the $(0001)\text{ZnO} \parallel (11\bar{2}0)\text{Al}_2\text{O}_3$ film; *b* — profile of the section along the indicated line.

Instead, the growth rate is limited by target destruction at high discharge current densities ($j > 120 \text{ mA/cm}^2$).

The reduction of epitaxy temperature to room levels and high growth rates are indicative of a specific crystallization mechanism of epitaxial ZnO films. In the present case, the substrate was located in the magnetron plasma region and charged by electrons with a surface density corresponding to a floating potential of 9–12 V [22]. This is likely to suppress bulk nucleation due to an increase in binding energy of charged adatoms with the substrate surface and violation of the condition for minimization of the formation energy of volume clusters of like-charged particles on the growth surface (two-dimensional growth). Forces acting between the same ions (adatoms) tangentially to the growth surface induce almost instantaneous ordering of matter, which translates into high growth rates.

Figure 3, *a* shows the microscopic image of a $5 \times 5 \mu\text{m}$ film region. The film has a fairly dense surface without voids or cracks. The section profile (Fig. 3, *b*) recorded in the

indicated film region revealed that the average particle size is close to 40 nm (this is also confirmed by the histogram of the particle size distribution). The average (R_a) and root-mean-square (R_q) roughness of the thin film were 10.7 and 13 nm, respectively.

Let us summarize the key results of the study.

- High growth rates of epitaxial ZnO films (up to 7 nm/s).

- Low epitaxy temperatures (35°C) at a film growth rate of 2.8 nm/s.

- The above parameters were achieved due to the optimal positioning of the substrate in the magnetron discharge region, which corresponded to a floating potential of 9–12 V on the substrate. As in the case of growth of highly oriented ZnO films on amorphous substrates [22], the floating potential on the substrate is regarded as the most critical technological parameter.

- The magnetron sputtering technique and technology may be scaled easily to produce zinc oxide films on large-

area substrates (2 inches or more). The obtained results may serve as a basis for industrial production of composite ZnO-on-sapphire substrates or free-standing ZnO substrates obtained by self-separation from a sapphire base (substrate).

This study was carried out within the State assignment of the Ministry of Science and Higher Education of the Russian Federation for the National Research Center „Kurchatov Institute“.

Conflict of interest

The authors declare that they have no conflict of interest.

References

- [1] F. Hadj-Larbi, R. Serhane, *Sensors Actuators A*, **292**, 169 (2019). DOI: 10.1016/j.sna.2019.03.037
- [2] W. Zhang, D. Jiang, M. Zhao, Y. Duan, X. Zhou, X. Yang, C. Shan, J. Qin, S. Gao, Q. Liang, J. Hou, *J. Appl. Phys.*, **125**, 024502 (2019). DOI: 10.1063/1.5057371
- [3] X.-L. Lu, X.-B. Guo, F.-C. Su, Z. Su, W.-H. Qiu, Y.-P. Jiang, W.-H. Li, Z.-H. Tang, X.-G. Tang, *J. Appl. Phys.*, **133**, 075301 (2023). DOI: 10.1063/5.0133534
- [4] K. Natu, M. Laad, B. Ghule, A. Shalu, *J. Appl. Phys.*, **134**, 190701 (2023). DOI: 10.1063/5.0169308
- [5] R. Triboulet, *Prog. Cryst. Growth Charact. Mater.*, **60**, 1 (2014). DOI: 10.1016/j.pcrysgrow.2013.12.001
- [6] P. Scajev, S. Miasojedovas, M. Mazuronyte, L. Chang, M.C. Chou, *J. Appl. Phys.*, **132**, 144501 (2022). DOI: 10.1063/5.0108890
- [7] J. Wang, P. Yang, *Vacuum*, **220**, 112844 (2024). DOI: 10.1016/j.vacuum.2023.112844
- [8] P. Gnanasambandan, N. Adjeroud, R. Leturcq, *J. Vac. Sci. Technol. A*, **40**, 062413 (2022). DOI: 10.1116/6.0001925
- [9] T.A. Heuser, C.A. Chapin, M.A. Holliday, Y. Wang, D.G. Senesky, *J. Appl. Phys.*, **131**, 155701 (2022). DOI: 10.1063/5.0077210
- [10] R. Triboulet, J. Perrière, *Prog. Cryst. Growth Charact. Mater.*, **47**, 65 (2003). DOI: 10.1016/j.pcrysgrow.2005.01.003
- [11] I.-S. Kim, S.-H. Jeong, S.S. Kim, B.-T. Lee, *Semicond. Sci. Technol.*, **19**, L29 (2004). DOI: 10.1088/0268-1242/19/3/L06
- [12] K.C. Ruthe, D.J. Cohen, S.A. Barnett, *J. Vac. Sci. Technol. A*, **22**, 2446 (2004). DOI: 10.1116/1.1807394
- [13] K. Kuwahara, N. Itagaki, K. Nakahara, D. Yamashita, G. Uchida, K. Kamataki, K. Koga, M. Shiratani, *Thin Solid Films*, **520**, 4674 (2012). DOI: 10.1016/j.tsf.2011.10.136
- [14] S.W. Shin, G.L. Agawane, I.Y. Kim, Y.B. Kwon, I.O. Jung, M.G. Gang, A.V. Moholkar, J.-H. Moon, J.H. Kim, J.Y. Lee, *Appl. Surf. Sci.*, **258**, 5073 (2012). DOI: 10.1016/j.apsusc.2012.01.109
- [15] S.H. Seo, H.C. Kang, *Mater. Lett.*, **98**, 131 (2013). DOI: 10.1016/j.matlet.2013.01.126
- [16] H.N. Riise, V.S. Olsen, A. Azarov, A. Galeckas, T.N. Sky, B.G. Svensson, E. Monakhov, *Thin Solid Films*, **601**, 18 (2016). DOI: 10.1016/j.tsf.2015.09.043
- [17] A. Akhmedov, A. Abduev, E. Murliev, A. Asvarov, A. Muslimov, V. Kanevsky, *Materials*, **14**, 6859 (2021). DOI: 10.3390/ma14226859
- [18] F. Arab, F. Kanouni, R. Serhane, Y. Pennec, *Mater. Today Commun.*, **38**, 107719 (2024). DOI: 10.1016/j.mtcomm.2023.107719
- [19] M.Z. Aslam, H. Zhang, V.S. Sreejith, M. Naghdi, S. Ju, *Measurement*, **222**, 113657 (2023). DOI: 10.1016/j.measurement.2023.113657
- [20] G. Fan, Y. Li, C. Hu, L. Lei, D. Zhao, H. Li, Z. Zhen, *Opt. Laser Technol.*, **63**, 62 (2014). DOI: 10.1016/j.optlastec.2014.04.001
- [21] T.D. Shermergor, N.N. Strel'tsova, *Plenochnyye p'ezoelektriki (Radio i Svyaz', M., 1986) (in Russian)*.
- [22] A.M. Ismailov, L.L. Emirasanova, M.Kh. Rabadanov, M.R. Rabadanov, I.Sh. Aliev, *Tech. Phys. Lett.*, **44**, 528 (2018). DOI: 10.1134/S1063785018060202.

Translated by D.Safin